This is a post-peer-review, pre-copyedit version of an article published in ARABIAN JOURNAL FOR SCIENCE AND ENGINEERING.The final authenticated version is available online at: http://dx.doi.org/10.1007/s13369-019-04074-4

Postprint of: Asrani, N.P., Murali, G., Abdelgader, H.S. et al. Investigation on Mode I Fracture Behavior of Hybrid Fiber-Reinforced Geopolymer Composites. Arab J Sci Eng 44, 8545–8555 (2019)

Investigation on Mode-I Fracture Behavior of Hybrid Fiber Reinforced Geopolymer Composites

Neha P Asrani[1], G. Murali[1], Hakim S. Abdelgader[2], K. Parthiban[1], M.K. Haridharan[3] and K. Karthikeyan[4]

[1] School of Civil Engineering, SASTRA Deemed to be University, India

[2] Visiting Professor at Gdansk University of Technology, Faculty of Civil and Environmental Engineering, Gdansk, Poland - Professor, Department of Civil Engineering, University of Tripoli, Tripoli, Libya.

[3] Assistant Professor (Senior grade), Amrita School of Engineering, Amrita Vishwa Vidyapeetham Deemed To Be University, India.

[4] Assistant Professor (Senior), SMBS, VIT Deemed University, Chennai campus, India.

Corresponding author email: murali@civil.sastra.edu, murali_220984@yahoo.co.in

Abstract

Recent reports in literature have shown that fiber reinforced geopolymer composites (FRGC) made with mono fibers exhibit a significant enhancement in fracture energy. However, many aspects of the fracture performance of hybrid fiber reinforced geopolymer composites (HFRGC) remain largely unexploited, and these are predominant for the structures. For the first time, the mode I fracture energy of HFRGC is investigated. The mode-I behavior was assessed using pre-notched beams in accordance with the RILEM three-point bending test. Five different HFRGC mixtures were prepared using three fiber types: steel, polypropylene, and glass (SF, PF and GF). The parameters of the pre-notched beam in flexure tested in this study were the first crack and peak load, crack mouth opening displacement (CMOD) at the first crack load and peak load, equivalent tensile strength, post-peak slope, reinforcing index, residual tensile strength, and fracture energy. The results reveal that there is a positive interaction amidst the fibers in geopolymer composites that leads to an enhancement in the mode-I fracture energy compared to the reference specimen. This study probes the influence of novel HFRGC while producing high-quality concrete, which can then be leveraged for sustainable infrastructure and various civil engineering works.

Keywords: Steel, Polypropylene, Glass, Geopolymer concrete, Fracture.

1. Introduction

Production of cement is associated with CO_2 emissions to the atmosphere, leading to causing the environment over the last two decades [1]. In an attempt to alleviate CO_2 emissions, the use of geopolymer binders has emerged as the newest wave of cement technologya and is a very favorable solution for reducing impact on ecosystem [2]. In recent years, geopolymer concrete has attracted the interest of researchers owing to its diverse merits, including the use of by-products [3], fire resistance [4], and alleviated CO_2 emissions [5],[6]. Geopolymers are attained through a chemical process between alkaline liquids and materials with high silica and alumina contents [7].

Despite their merits, geopolymer composites exhibit more brittleness compared to conventional concrete [8]. The incorporation of fibers to geopolymer composites has the potential to alleviate its brittleness and enhance its ductility [9],[10]. For this reason, many researchers have revealed the mechanical properties of FRGC prepared with various fibers [11],[12],[13],[14]. Nevertheless, there still exists a large knowledge gap on the fracture performance of FRGC, particularly with hybrid fibers. Recent research has explored the mode-I fracture performance of fiber reinforced composites (FRC) with mono fibers [15],[16],[17],[18],[19], while hybrid fibers consisting of two or three fiber types have been largely unexplored by researchers, especially in geopolymer concrete.

For instance, Yao et al. [20] explored the properties of FRC containing carbon, polypropylene, and steel fibers and reported that the flexural toughness and strength characteristics were enhanced with the steel–carbon hybrid. In addition to improving the fracture toughness, incorporation of hybrid fibers in the concrete also significantly enhanced the durability. This immense increase in durability is a function of the high ductility, fineness, and dispersion that hinders plastic cracking [21],[22]. Ganesan et al. [23]

revealed that the utilization of hybrid fibers could enhance several engineering aspects, including the ductility factor, first crack, and ultimate load characteristics. Use of steel fiber has proven to be more beneficial than polypropylene fiber in terms of ductility. Banthia and Soleimani [24] examined fiber reinforced geopolymer composites hybrid fibrous cementitious composites made with amalgamations of carbon, polypropylene, and steel fibers. It was concluded that a better three-fiber hybrid was formed with an extensively deformed geometry of mono steel fibers than with a less deformed geometry. Almusallam et al. [25] explored the mode-I fracture behavior of hybrid fibrous concrete made with amalgamations of different fibers, including steel, Kevlar, and polypropylene fibers. The results showed that an increment in the steel fiber dosage led to enhanced fracture properties of the hybrid fibrous concrete mixes. Rooholamini et al. [26] examined the mode-I fracture behavior of roller-compacted fibrous concrete made with different types and lengths of mono and hybrid fibers. The results showed that hybrid fibers (steel + micro polypropylene) exhibited the lowest toughness, while mono steel fiber was dominant in bridging macro-cracks, resulting in a substantial enhancement in the post-cracking curve. Alberti et al. [27] examined the flexural and uniaxial fracture performance of polyolefin and hooked-end steel fibers in their separate and hybrid forms. The results demonstrated that the residual strength, toughness, and fracture characteristics were enhanced in the hybrid form to a greater extent than the same amount of fibers added individually. This shows that there is a synergic effect between the fibers, which opens a wide area that must be examined in future. This synergy between fibers gave rise to high-performance concrete, which is effective in resisting loads near the ultimate load for a deflection of span/60. However, data on the mode-I fracture performance of HFRGC have scarcely been reported at present.

2.0 Research Significance

Although fracture behavior of mono fiber geopolymer composites has been explored by many researchers in recent years, work on HFRGC still needs special emphasis. This has motivated the experimental investigation in this study, which pioneers the influence of HFRGC with superior fracture energy. This is accomplished using three fibers types: steel, polypropylene, and glass with different dosage.

3.0 Experiential campaign

3.1 Materials

The material utilized to produce the HFRGC was (Ground-granulated blast-furnace slag) GGBS, the alkaline activator, coarse and fine aggregate and fibers. The alkaline liquid consisted of a 12 Molarity solution of NaOH and Na_2SiO_3. Sodium hydroxide flakes were dissolved in distilled water to prohibit the consequences of indefinite adulteration in the mixing water. To obtain a homogenous solution, the NaOH mixture was prepared a day before its utilization in the concrete preparation. The optimum percentage of geopolymer mix and water-to-binder ratio were selected based on previous studies [28],[29]. The coarse aggregate was a locally available gravel with sizes of 12.5 and 20 mm obtained from the Thanjavur area; the fine aggregate used was superior quality river sand. The fineness modulus and specific gravity of M-sand were 2.83 and 2.6 respectively. The ingredients utilized in the mix design of the HFRGC are enumerated in Table 1. All the mixes were cured at ambient temperature to utilize samples cast under in-situ conditions. Three dissimilar fibers were utilized in this research: 5D hooked-end SF, PF and GF. The configuration of the fibers used in this research is exemplified in Fig. 2, and the fiber properties are summarized in Table 2. A set of four mixes were prepared to investigate the effect of hybrid fibers on the mode-I fracture performance of HFRGC compared to that of a reference mix (M0). Three mixes were prepared with combination of two fibers at dosages of 1.6% (1.3% of SF and 0.3% GF), 1.6% (1.3% of SF and 0.3% of PF), and 0.6% (0.3% of PF and 0.3% of GF). Additionally, the final mix was prepared using a three fiber combination at a dose of 1.6% (1.0% of SF, 0.3% of PF and 0.3% of GF). A fiber dosage of more than 1.6% causes uneven distribution with a vulnerability to conglobate, leading to inner defects and weak in interfacial transition zones that ultimately cause a reduction of strength. These hybrid

fiber combinations were obtained to make sure that the maximum fiber dosage was limited to 1.6% to avoid fiber agglomerating. The fibers were added as a percentage (volume fraction) based on the total volume of concrete. The mixtures used 100% GGBS as the aluminosilicate source, which significantly shortens the setting time compared to using fly ash. The mixtures had extremely low workability and very short setting times owing to their composition consisting of 100% GGBS, 1.6% fibers, and a liquid/binder ratio of 0.5. The fiber dosage of 1.6% is very high, especially when the fine PP and GF fibers are used; these fibers have very high surface areas that absorb the liquid. This substantially diminishes the workability of the mixtures, but improves their density, compressive strength, and fracture energy.

3.2 Test configuration and instrumentation

To evaluate the compressive strength, 150 mm cubic samples were fabricated and tested in accordance with IS 516 [30]. The average results of the three samples prepared from each mix is presented. The fracture tests on centrally pre-notched beams were performed according to RILEM [31], as shown in Fig. 3. The properties assessed in the laboratory tests include the first crack load and peak load, CMOD at the first crack load and peak load, equivalent tensile strength, post-peak slope, residual tensile strength, reinforcing index, and fracture energy, according to the guidelines given in RILEM [31]. For centrally pre-notched beams with similar geometry (150 mm × 150 mm × 600 mm), the notch thickness, notch-to-depth ratio, and span-to-beam depth ratio are 5 mm, 0.167, and 3, respectively. All of the beams were loaded at a rate of 0.05 mm/min under three-point bending with a span of 450 mm (see Fig. 3). A load cell, linear variable displacement transducer (LVDT), and portable microscope were installed to calculate the load, deflection, and CMOD, respectively (see Fig. 4). The CMOD was observed using a high-magnification crack microscope with a precision of 0.01 mm. Images were recorded at regular intervals until failure of the beam. The mid-span vertical deflection was assessed in the proximity of the lower side of the pre-notched beam using a LVDT. The fracture energy, $U_{f,}$, can be evaluated using the formula suggested in [32],[33],[34],[35] as follows:

$$U_f = \frac{P_0 + mg\delta_f}{A_l} \qquad (1)$$

where P_o is the area beneath the full-load deflection curve; m is the mass of the beam with a span of 450 mm; g is the gravitational acceleration; A_l denotes the area of ligament, calculated as $A_l = b\ h_e$, in which h_e is the effective depth of the beam $(=h\text{-}a_o)$, and b, d, and a_o represent the breadth, depth, and notch depth of the beam, respectively; δ_f is the maximum recorded deformation.

4. Discussion of results

4.1 X-ray diffraction

The dissolution of the solid particles and the geopolymerization reaction can be effectively increased by using an activator solution (i.e., sodium hydroxide solution) of higher concentration, which will result in improved mechanical properties through the increased leaching of Si and Al atoms. In addition, the greater amount of reaction heat evolved at higher concentrations may lead to improved dissolution of the source material. Hence, an activator solution consisting of a 12 M sodium hydroxide solution mixture with a ratio of sodium silicate solution to sodium hydroxide solution of 2.0 was utilized in this study to dissolve the GGBS utilized as the source material.

Figure 5 shows the X-ray diffractogram for the resulting mix after curing under ambient conditions to an age of 287 d. The formation of calcite and scolecite ($CaAl_2Si_3O_{10}{\cdot}3H_2O$) as reaction products can be observed in addition to the presence of partially unreacted silica. The existence of scolecite results in the presence of calcium aluminosilicate hydrate (C-(A)-S-H) rather than sodium aluminosilicate hydrate (N-(A)-S-H) due to the utilization of GGBS with a high calcium content. The amorphous nature of the mix in the range of 2θ = 28°–34° is also observed; this may be due to the ambient curing, whereas a crystalline product would have been formed during curing at elevated temperature, which may result in a greater degree of leaching.

4.2 Compressive strength of HFRGC

The compressive strength of HFRGC comprising different fiber combinations is shown in Fig. 6. From the Fig. 6, the fibrous geopolymer composites contain two or three combinations of fibers. The obtained compressive strengths for mixtures M1, M2, and M3 were 27.5%, 24.8%, and 16.3% higher, respectively, than that for mix M0. Careful observation of Fig. 6 reveals that the combinations of three fibers led to a compressive strength that was 20.5% higher than that of M0. Specimen M1 displayed greater compressive strength than specimen M4, which can be attributed to the presence of a 1.3% dosage of SF and 0.3% dosage of GF in specimen M1. The intrinsic increase owing to the presence of the combination of two fibers in the hybrid FGC, which plays a significant role in arresting crack development by merging the cracks (micro and macro) in the tension zone. Generally, the primary reason for rise in the compressive strength of mixture M1 is due to the capability of uniformly distributed SF and GF to restrict the propagation of cracks (micro and macro), thus alleviating the stress concentration and leading to more uniform stress in the concrete; changes in the path of the cracks is accountable for bridging and fibers, leading to a suspension in the crack growth rate [38]. A higher compressive strength in the crack zone is provided by the M1 mixture, followed by the combination M2 mixtures, as a consequence of limited crack propagation and adjoining crack tips.

4.3 Load–CMOD (P–CMOD) curves

The experimental results and evaluated fracture energies are enumerated in Tables 3 and 4, respectively.

Figure 7 shows the P–CMOD curves for the HFRGC notched beam (M1). The P–CMOD curves in Figs. 7 and 8 clearly illustrate the outcome of hybrid fibers on the post-behavior of geopolymer composites. For the M0 mixture, the first crack and ultimate load occurred at approximately 14.2 kN and 17.4 kN, respectively. From the curve, the CMOD values at the first crack and peak load were 0.02 mm and 0.03 mm, respectively, which was considered insignificant. The M0 beam immediately collapsed upon reaching its ultimate load, which is the reason for the absence of a descending branch of the curve. On the other hand, the response of the HFRGC exhibited a substantial difference in the shapes of the P–CMOD curves: smaller descending branches were observed and no beams collapsed, which was considered a good outcome. The maximum ultimate load carrying capacities for beams M1, M2, M3, and M4 were 61.9 kN, 53.0 kN, 36.2 kN, and 58.1 kN, respectively, and the corresponding CMOD values were 1.1, 1.3, 1.4, and 1.2 mm, respectively, which are 255.7%, 204.6%, 108.0%, and 233.9% higher than that of the M0 beam, respectively.

This can be ascribed to the crack-bridging fibers that constantly transmit the tensile stress across the cracks zone until fiber pull-out occurs, leads to higher first crack and ultimate loads. In addition, this crack-bridging property influences the crack stabilization mechanism, as it drastically improves the load carrying capacity. This mechanism plays a vital role in resisting CMOD through fiber de-bonding, slipping, and pull-out, together with postponing the crack propagation. It is worth noting that matrix failure occurs on macro and micro scales, and hybrid fibers have been shown to limit the growth and spread of cracks that improve the post-cracking ductility [39],[40]. For hybrid fiber reinforced concrete, different fibers control cracks at varying scales and strain limits. This has no effect on crack control at other scales [40]. In hybrid fiber concrete, every fiber has a distinct role in the crack-bridging mechanism. For a similar volume fraction of fibers, PF and GF are more effective at hindering micro-crack initiation and propagation because they are thinner and more numerous than SFs. Micro-fibers also enhance the pull-out behavior of SFs, leading to increased toughness [41]. Because micro-cracks coalesce to form macro-cracks, SFs become more effective for controlling crack development. Hence, the tensile toughness and ductility are improved [42]. Furthermore, this leads to a reduction in the crack opening, thereby influencing the post-peak flexural softening and apparently changing the slope of the P–CMOD curves of HFRGC, which is fairly slight.

4.4 Load–deflection (P–δ) curves

The (P–δ) curves for the HFRGC beams are shown in Fig. 9. For beam M0, the beam reaches its ultimate loading capacity after the load is dramatically decreased. From the other point of view, the HFRGC beams exhibited superior post-cracking behavior and had a

much larger area under the P–δ curve than the control composite (M0). The same trend was also stated in earlier studies [25]. This can be ascribed to the fact that the fracture energy is directly in proportion to the area beneath the P–δ curve and the maximum δ of the beams. The deflections at the peaks for beams M1, M2, M3, and M4 were 1, 1, 1.3, and 1.2 mm, respectively. Strain softening performance was noticed with further increase in the load, leading to the descending branch of the curve. For the HFRGC beams, the softening performance can be identified by linear decrease with a slope of between 2.36 and 3.56 kN/mm. Owing to the high fiber dosage in the hybrid combinations, the matrix fiber bonding was strong, resulting in a controlling criterion for arresting cracks.

4.5 Reinforcing index

The fiber dosage, fiber properties, fiber geometry, fiber aspect ratio, and matrix properties all influence the cracking behavior of HFRGC [35],[36],[37],[38]. The fiber reinforcing index (RI) concept was introduced by Ezeldin and Balaguru [38] to rationalize the stress–strain curve parameters for hooked-end steel FRC. This concept was extended in subsequent studies [43],[44] for the creation of stress–strain curves for fibre reinforced concrete incorporated with crimped steel. However, SF alone was used in these studies [38],[43],[44]. In later studies, conceptualization of the RI was further extended to hybrid FRC [45]. The RI can be expressed as follows [38]:

$$RI = \sum_i^n RI_i \qquad (2)$$

where i corresponds to the fiber type and has a value of 1 for SF, 2 for PF, and 3 for GF; RI_i indicates the RI value for the i^{th} material, which was rationalized from the earlier model [45],[46] to include the tensile strength effect of the fibers, as follows:

$$RI = V_{fi}\frac{B_i L_i}{D_i}\left(\frac{T_{im}}{T_{sf}}\right)^w \qquad (3)$$

where V_{fi} denotes the fiber dosage; B_i represents the fiber bond factor, which is considered in this study to have values of 1, 1, and 0.1 for SF, PF, and GF, respectively; L_i denotes the length of fiber; D_i denotes the diameter of fiber; T_{im} represents the tensile strength of the material of the i^{th} fiber; T_{sf} is the tensile strength of SFs; and w is a tension stiffness parameter, which is as assigned a value of 0.5. The RI for the evaluation of the post-cracking performance of HFRGC is attained with the theory that the fiber content at the pre-notched zone is equal to the given fiber content for the beam. The calculated RI values for the HFRGC specimens are listed in Table 4.

4.6 Flexural tensile strength (FTS)

A comparison of the FTS of HFRGC specimens is summarized in Table 4, and the results reveals that the values are comparable to that for M0. A large increase in the FTS was observed with the inclusion of two or three fiber types in the geopolymer composites. For instance, the FTS for composites M1, M2, M3, and M4 were improved by 250.0%, 199.8%, 104.7%, and 228.6%, respectively, as compared to M0 beam. This discloses a substantial enhancement in the post-cracking efficiency of hybrid fibers in geopolymer composites relative to the control beam (M0). The FTS can be evaluated using the following equation:

$$FTS = \frac{3P_{max}L}{2b(h-a_0)^2} \qquad (4)$$

where L is the effective span of the beam, and P_{max} is the peak load.

4.7 Equivalent tensile strength

Based on the equation given in RILEM [31], two equivalent tensile strength (f_a and f_b) values were determined from the typical P–δ curve at different deflection points to design at the limit state of serviceability; the method is self-explanatory. Fig. 10 (a) and (b) shows the selected deflection points from the experimental P-δ curve used to calculate the equivalent tensile strength of HFRGC. The two equivalent tensile strengths, f_a and f_b, based on the energy absorption capacity for the area under the P–δ curve were assessed up to deflections of δ_2 and δ_3 ($\delta_2 = \delta_L + 0.65$ and $\delta_3 = \delta_L + 2.65$, where δ_L is the deflection at ultimate load), respectively. It is worth noting that the fraction corresponding to the energy required for the fracture of the control beam was excluded, and only the effect of the fibers on the fracture energy absorption performance was considered in calculation of the equivalent tensile strength HFRGC, as shown in Fig. 10 (a) and (b). Thus, f_a and f_b were determined using Eqs. (5) and (6), respectively [47],[48],[49].

$$f_a = \frac{3L}{2b(h-a_0)^2}\left(\frac{A_1}{0.5}\right) \qquad (5)$$

$$f_b = \frac{3L}{2b(h-a_0)^2}\left(\frac{A_2}{2.5}\right) \qquad (6)$$

f_a and f_b are the equivalent flexural strengths based on the energy absorption capacity for areas A1 and A2 under the P–δ curve ending at deflections of δ_2 and δ_3, respectively.

4.8 Residual tensile strength

Figure 11 illustrates the assessment of the group-wise deviations in the residual tensile strength (f_i) according to recent guidelines [50], which provides knowledge about the outline of the declining branch of the P–CMOD curves. However, previous studies [47] have demonstrated that f_i for HFRGC is comparatively more vulnerable to local irregularities in the P–CMOD curves. Obviously, in terms of strength at $CMOD_1$, the M1, M2, and M4 HFRGC beams exhibited higher strengths than the control beam (M0). This trend was clear for HFRGC beams owing to the presence of SF, which resists pull-out from the composites under a flexural tensile load. Moreover, these values increased up to $CMOD_2$, and then decreased beyond that point ($CMOD_1$ – $CMOD_4$). The residual tensile strength can be calculated using Eq. (7).

$$f_i = \frac{3P_iL}{2b(h-a_0)^2} \qquad (7)$$

4.9 Fracture absorption under mode-I

The fracture energy and associated properties are enumerated in Table 4. The fracture energy absorption of the control beam was 0.025 N/mm. In terms of the influence of the fibers and fiber dosage, this value was increased with hybrid fiber combinations, reaching 15.72 N/mm in HFRGC beams. The fracture energy absorption was 15.72 N/mm for beam M1, 13.25 N/mm for beam M2, 9.80 N/mm for beam M3, and 14.90 N/mm for beam M4. Comparing the highest fracture energies for the HFRGC beams, beam M1 containing 1.3% SF and 0.3% GF was greater compared to the other HFRGC beams: 18.6% greater than M2, 60.4% greater than M3, and 5.5% greater than M4. These results reveal that the geopolymer composite reinforced with 1.3% SF + 0.3% GF exhibited the highest fracture energy resistance, followed by hybrid combination of 1.3% of SF together with 0.3% of PF and 0.3% GF. The control beam, M0, had a small fracture energy and exhibited ductile behavior owing to the absence of post-peak descending curve in the P–δ curve. It is clear that the inclusion of hybrid fibers provided substantial enhancements in both the fracture energy and maximum deflection of geopolymer composites.

An even distribution of fibers can facilitate crack bridging and provide effective reinforcement in the matrix. A strong adhesive bond between the matrix and the fibers can transfer stresses from the tip of the crack to its upper and lower surfaces. This is highlighted in Fig. 12. The extent of the stress concentration is thus reduced, and the matrix develops a uniform stress. This in turn enhances the fracture toughness. However, a large amount of fibers result in poor dispersion and conglobation, leading to weaker interfacial transition zones and higher internal flaws, thus causing a loss of the fiber reinforcement effect.

Figure 13 shows the failure patterns for plain and HFRGC beams under mode-I fracture testing. The results show that both concrete mixes exhibit fracture paths that continue from the initial crack frontage when subjected to symmetric pure mode-I loading conditions. In the HFRC beam, there was a progressive crack build-up after the initial fracture at the tip, whereas the plain concrete displayed a quick, brittle, and sudden failure. Hybrid fibers play a major role in hindering swift sudden crack opening. Hence, the addition of hybrid fibers in geopolymer composites can significantly enhance the energy needed for the rupture of HFRGC specimens. In mode-I loading, discretionarily aligned fibers located almost perpendicular to the fracture propagation surface are exposed to direct tensile loads. The HFRGC shows a strong post-fracture behavior that can be attributed to the exemplary tensile stiffness of the hybrid fibers (SF + GF + PF). Moreover, hybrid fibers noticeably improve the post-failure tensile load bearing capacity, as shown in Fig. 13. In

general, fracture energy is calculated from the beginning of cracking to the final failure of the HFRGC specimens, determined from the area under the (P–δ) curves.

5.0 Conclusions

The paper presents the Mode-I fracture performance of HFRGC; the influence of hybrid fibers is evaluated. The Mode-I fracture performance was experimentally evaluated using RILEM three-point bending, tests for plain and HFRGC with different fiber combinations and dosages. From the discussion of results, the subsequent conclusions can be made:

1. There is a considerable enhancement in the efficiency of hybrid fibers in geopolymer composites, especially with SF, which plays a crucial role in arresting crack development and propagation by connecting macro-cracks. GF and PF bridge the micro-cracks in the tension zone.
2. The maximum compressive strength was attained for specimen M1, followed by M2, M4, and M3. The obtained compressive strengths for mixtures M1, M2, and M3 were 27.5%, 24.8%, and 16.3% higher, respectively, than that for mix M0. This can be ascribed to even distribution of SF and GF to limit the extension of cracks (micro and macro), alleviating the stress concentration at particular zone and resulting in more uniform stress distribution in the composites.
3. The maximum ultimate load carrying capacities of beams M1, M2, M3, and M4 were 255.7%, 204.6%, 108.0%, and 233.9% higher, respectively, than that of beam M0, and the corresponding CMOD values were 1.1, 1.3, 1.4, and 1.2 mm, respectively. This increase in ultimate load owing to the crack-bridging fibers (SF + GF + PF) that constantly transmit the tensile stress across the cracks until fiber pull-out occurs.
4. For the HFRGC investigated under RILEM three-point bending, a optimistic interaction between the hybrid fibers in HFRGC that led to an enhancement in the fracture energy up to 15.72 N/mm compared to the reference specimen. The hybrid combination of GF and PF resulted in a lower fracture energy, SF with PF or GF is the most effective for bridging micro- and macro-cracks, ensuring the ability to attain hardening of the post-cracking curve owing to increased stiffness.
5. The control beam (M0) exhibited quick and brittle failure, while the HFRC beams demonstrated superior ductile behavior as a result of the bridging action of hybrid fibers. The production of geopolymer composites incorporating SF, GF, and PF fibers can be utilized efficiently to make eco-friendly composites that increase the fracture energy and other properties to a significant extent.

Further study may be needed to enlarge the present investigation by considering different fibres (3D and 4D hooked end, crimped, hybrid, recycled and basalt) with different aspect ratios and different concrete (recycled aggregate concrete, recycled tyre rubber concrete, light and heavy weight concrete and green concrete) could be the scope for the future study.

Acknowledgements

Authors grateful to SASTRA University for the support.

Compliance with Ethical Standards

Conflict of interest

The authors declares that they have no conflict of interest.

Table 1 Mix proportion quantities per cubic meter

Mix ID	GGBS (kg/m^3)	FA (kg/m^3)	CA (kg/m^3)	W/B Ratio	NaOH (kg/m^3)	Na_2SiO_3 (kg/m^3)	SF (%)	PP (%)	GF (%)
M0	414	515	956	0.5	69	138	0	0	0
M1	414	515	956	0.5	69	138	1.3	0	0.3

M2	414	515	956	0.5	69	138	1.3	0.3	0
M3	414	515	956	0.5	69	138	0	0.3	0.3
M4	414	515	956	0.5	69	138	1	0.3	0.3

FA: Fine aggregate, CA: Coarse aggregate

Table 2 Fibers properties.

Properties	SF	GF	PF
Length (mm)	60	15	13
Diameter (mm)	0.9	1	0.095
Tensile Strength (MPa)	1050	1400	360

Table 3 Experimental test results

Mix ID	Compressive strength (MPa)	Load at first crack (kN)	CMOD at first crack (mm)	Load at Peak (kN)	CMOD at peak load (mm)	Post-peak slope (up to ~7.5 mm) (kN/mm)
M0	62.41	14.2	0.02	17.4	0.033	0
M1	79.56	22.3	0.02	61.9	1.1	-3.56
M2	77.88	18	0.02	53	1.3	-3.194
M3	72.59	15.1	0.03	36.2	1.4	-2.366
M4	75.20	20.5	0.02	58.1	1.2	-3.508

Table 4 Evaluated fracture properties

Mix ID	RI	U_f up to $CMOD_4$, (N/mm)	FTS (MPa)	Equiv. tensile strength (MPa)		Residual tensile strength (MPa)				U_f (N/mm)
				f_a	f_b	$f_{R,1\text{-}CMOD}$	$f_{R,2\text{-}CMOD}$	$f_{R,3\text{-}CMOD}$	$f_{R,4\text{-}CMOD}$	
M0	0	0.025	5.09	-	-	-	-	-	-	0.025
M1	0.87	10.28	17.82	18.28	16.01	13.84	17.04	15.98	14.30	15.72
M2	1.03	7.72	15.26	17.86	13.59	13.13	15.06	16.87	12.29	13.25
M3	0.16	4.92	10.42	15.20	10.63	5.76	8.30	7.77	6.90	9.80
M4	0.83	9.92	16.73	21.53	16.24	13.3	16.5	15.6	14.45	14.90

Fig. 1 Mixing of the HFRGC

(a) Steel (b) Glass (c) Polypropylene

Fig. 2 Configuration of the fibers

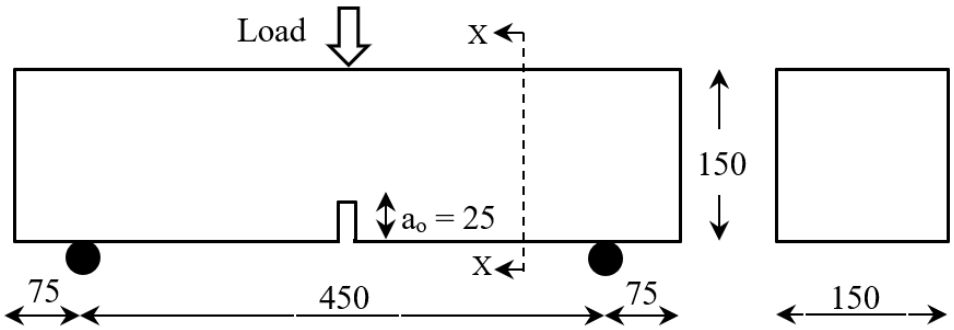

Fig. 3 Geometry of the pre-notched beam (all dimensions are in mm)

Fig. 4 Mode-I fracture test setup

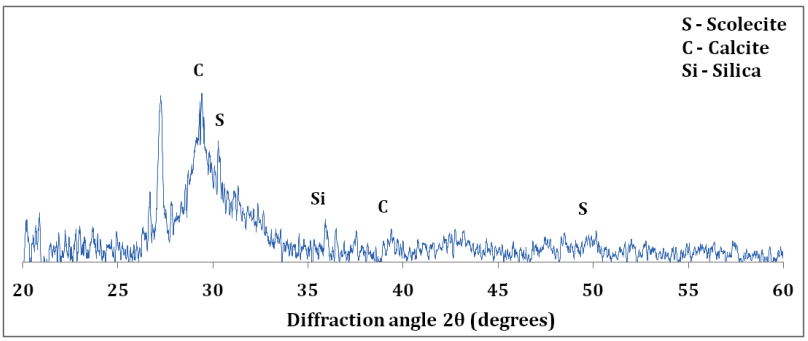

Fig. 5 X-ray diffraction pattern of the geopolymer composite [1].

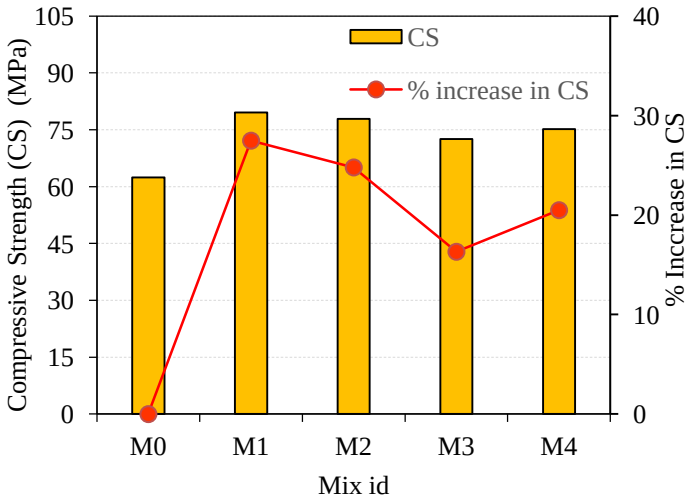

Fig. 6 Compressive strengths of HFRGC mixtures

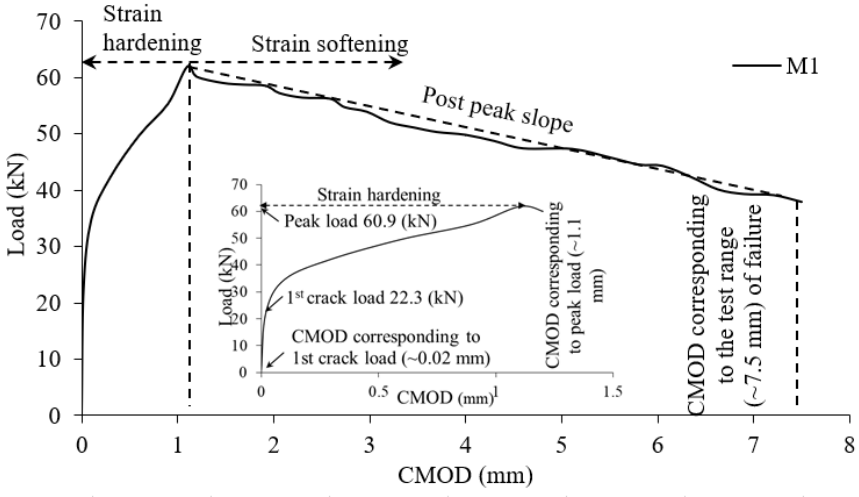

Fig. 7 Load–CMOD curve for the M1 HFRGC beam

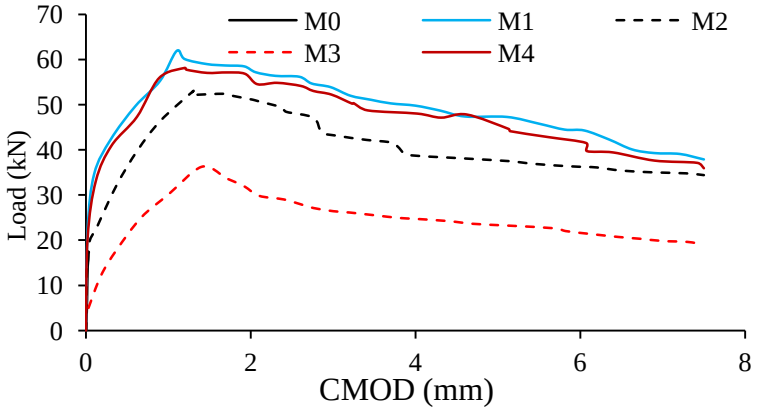

Fig. 8 Load–CMOD curve for the control and HFRGC beams

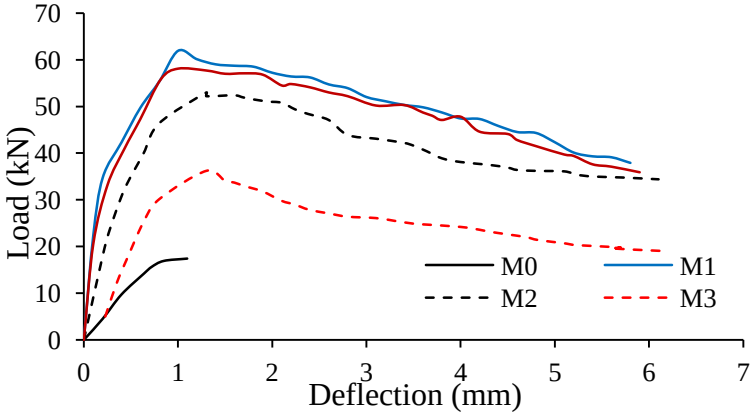

Fig. 9 (P–δ) curves for the control and HFRGC beams

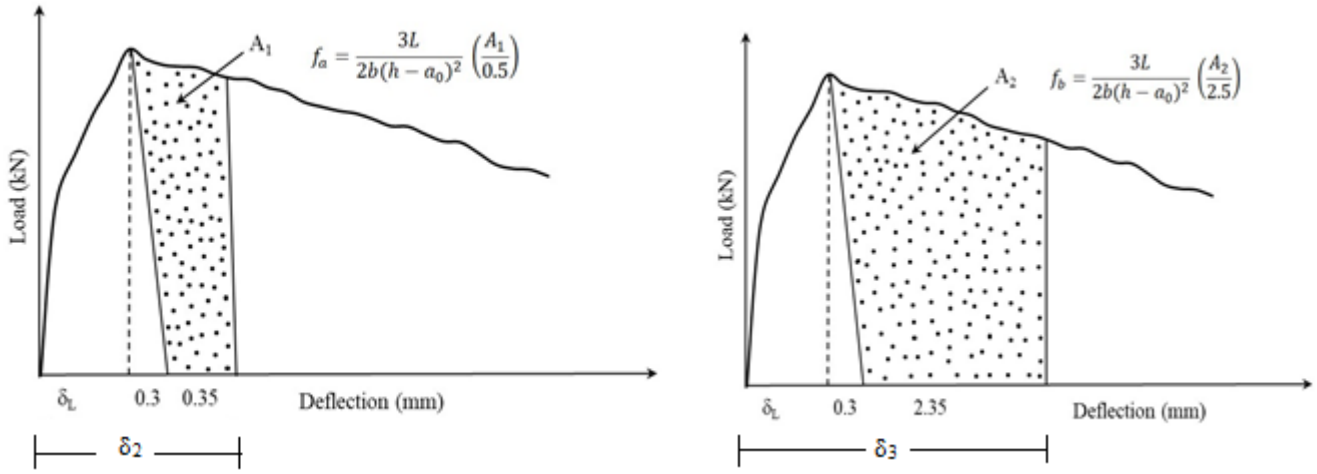

(a) (b)

Fig. 10 Assessment of FTS based on RILEM TC 162-TDF [32]: (a) f_a and (b) f_b

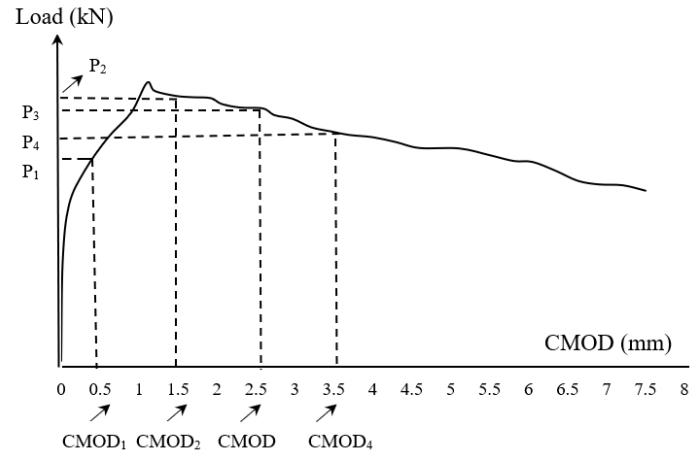

Fig. 11 Assessment of the residual tensile strength according to RILEM based on the standard CMOD values [32]

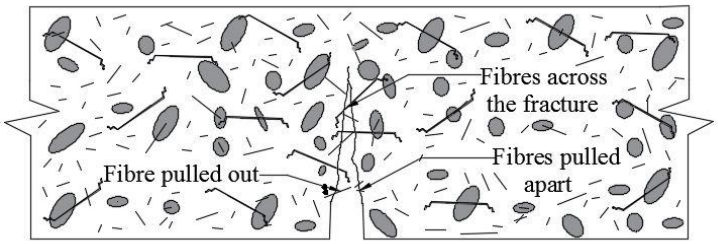

Fig. 12 Fiber distribution in the fracture zone

Fig. 13 Failure patterns for beams M0 and M4

References

[1] Neha P Asrani,: Murali, G.: Parthiban, K.: Surya, K.: Prakash, A.: Rathika, K.: Uma Chandru.: A feasibility of enhancing the impact resistance of hybrid fibrous geopolymer composites: Experiments and modelling. Constr Build Mater. **203**, 56–68 (2019).

[2] Maa, C.K.: Awang, A.Z.: Omar, W.: Structural and material performance of geopolymer concrete: A review. Constr Build Mater. **186**, 90–102 (2018).

[3] Sakulich, A.R.: Reinforced geopolymer composites for enhanced material greenness and durability. Sustainable Cities Soc. **1 (4)**, 195–210 (2011).

[4] Benhalal, E.: Zahedi, G.: Shamsaei, E.: Bahodori, A.: Global strategies and potentials to curb CO_2 emissions in cement industry. J Clean Prod. **51**, 142–161 (2012).

[5] Al-Majidi, M.H.: Lampropoulos, A.: Cundy, A.B.: Tensile properties of a novel fibre reinforced geopolymer composite with enhanced strain hardening characteristics. Composite Structures, **168**, 402–427 (2017).

[6] Deb, P.S.: Nath, P.: Sarker, P.K.: The effects of ground granulated blast-furnace slag blending with fly ash and activator content on the workability and strength properties of geopolymer concrete cured at ambient temperature. Mater Des. **62 (10)**, 32–39 (2014).

[7] Patil, K.K;: Allouche, E.N.: Impact of Alkali Silica Reaction on Fly Ash-Based Geopolymer Concrete. J Mater Civ Eng. **25(1)**, 131-139 (2013).

[8] Sukontasukkul, P.: Pongsopha, P.: Chindaprasirt, P.: Songpiriyakij, S.: Flexural performance and toughness of hybrid steel and polypropylene fibre reinforced geopolymer. Constr Build Mater, **161**, 37–44 (2018).

[9] Noushini, A.: Hastings, M.: Castel, A.: Aslani, F.: Mechanical and flexural performance of synthetic fibre reinforced geopolymer concrete, Constr Build Mater. **186**, 454–475 (2018).

[10] Majidi, M.H.A.: Lampropoulos, A.: Cundy, A.B.: Steel fibre reinforced geopolymer concrete (SFRGC) with improved microstructure and enhanced fibre-matrix interfacial properties. Constr Build Mater. **139**, 286–307 (2017).

[11] Nematollahi, B.: Sanjayan, J.: Shaikh, F.U.A.: Comparative deflection hardening behavior of short fiber reinforced geopolymers composites. Constr Build Mater, **70(15)**, 54-64 (2014).

[12] Shaikh, F.U.A.: Deflection hardening behavior of short fiber reinforced fly ash based geopolymer composites. Mater Des. **50**, 674-82 (2013).

[13] Nematollahi, B.: Sanjayan, J.: Shaikh, F.U.A.: Matrix design of strain hardening fiber reinforced engineered geopolymer composite. Compos Part B Eng. **89**, 253-65 (2015).

[14] Korniejenko, K.: Fraczek, E.: Pytlak, E.: Adamski, M.: Mechanical properties of geopolymer composites reinforced with natural fibers. Procedia Eng. **151**, 388-93 (2016).

[15] Kabay, N.: Abrasion resistance and fracture energy of concretes with basalt fiber. Constr Build Mater. **50**, 95–101 (2014).

[16] Lee, J.: Lopez, M.M.: An Experimental Study on Fracture Energy of Plain Concrete. Inter J Concr Struct Mater. **8 (2)**, 129–139 (2014).

[17] Bideci, A.: Öztürk, H.: Bideci, Ö.S.: Emiroglu, M.: Fracture energy and mechanical characteristics of self-compacting concretes including waste bladder tyre. Constr Build Mater. **149**, 669–678 (2017).

[18] Kumar, S.S.: Pazhani, K.C.: Ravisankar, K.: Fracture behaviour of fibre reinforced geopolymer concrete. Current Science. **113 (1)**, 116-122 (2017).

[19] Xie, J.: Huang, L.: Guo, Y.: Li, Z.: Fang, C.: Li, L.: Wang, J.: Experimental study on the compressive and flexural behaviour of recycled aggregate concrete modified with silica fume and fibres. Constr Build Mater. **178**, 612–623 (2018).

[20] Yao, W.: Li, J.: Keru, W.: Mechanical properties of hybrid fiber-reinforced concrete at low fiber volume fraction. Cem Concr Res. **33(1)**, 27–30 (2003).

[21] Sivakumar, A.: Santhanam, M.: A quantitative study on the plastic shrinkage cracking in high strength hybrid fibre reinforced concrete. Cem Concr Compos, **29 (7)**, 575–581 (2007).

[22] Hsie, M.: Chijen, T.: Song, P.S.: Mechanical properties of polypropylene hybrid fiber-reinforced concrete. Mater Sci Eng, **A 494 (1-2)**, 153–157 (2008).

[23] Ganesan, N.: Indira, P.V.: Sabeena, M.V.: Behaviour of hybrid fibre reinforced concrete beam–column joints under reverse cyclic loads. Mater Des, **54**, 686–693 (2014).

[24] Banthia, N.: Soleimani, S.M.: Flexural response of hybrid fiber reinforced cementitious composites. ACI Materials Journal, **102(6)**, 382–389 (2005).

[25] Almusallam, T.: Ibrahim, S.M.: Al-Salloum, Y.: Aref Abadel.: Abbas, H.: Analytical and experimental investigations on the fracture behavior of hybrid fiber reinforced concrete. Cem Concr Composites, **74**, 201-217 (2016).

[26] Rooholamini, H.: Hassani, A.: Aliha, M.R.M.: Fracture properties of hybrid fibre-reinforced roller-compacted concrete in mode I with consideration of possible kinked crack. Constr Build Mater. **187**, 248–256 (2018).

[27] Alberti, M.G.: Enfedaque, A.: Gálvez, J.C.: Fibre reinforced concrete with a combination of polyolefin and steel-hooked fibres. Composite Structures, **171**, 317–325 (2017).

[28] Parthiban, K.: Kaliyaperumal, S.R.M.: Influence of recycled concrete aggregates on the flexural properties of reinforced alkali activated slag concrete. Constr Build Mater. **102(1)**, 51-58 (2016).

[29] Parthiban, K.: Kaliyaperumal, S.R.M.: Influence of recycled concrete aggregates on the engineering and durability properties of alkali activated slag concrete. Constr Build Mater. **133**, 65-72 (2017).

[30] IS: 516-1959. Indian standard method of tests for strength of concrete. Reaffirmed 2004.

[31] RILEM TC 162-TDF L. Vandewalle, et al.: Test and design methods for steel fibre reinforced concrete bending test, materials and structures, RILEM Publications. Mater Struct, **35**, 579-582 (2002).

[32] Al-Tayeb, M.M.: Abu Bakar, B.: Akil, H.M.: Ismail, H.: Effect of partial replacements of sand and cement by waste rubber on the fracture characteristics of concrete. Polym Plast Technol Eng, **51 (6)**, 583–589 (2012).

[33] Güneyisi, E.: Gesoglu, M.: Özturan, T.: Ipek, S.: Fracture behavior and mechanical properties of concrete with artificial lightweight aggregate and steel fiber. Constr Build Mater. **84**, 156–168 (2015).

[34] Malvar, L.J.: Warren, G.: Fracture energy for three-point-bend tests on single edge- notched beams. Exp Mech, **28 (3)**, 266–272 (1988).

[35] RILEM FMC-50, Determination of the fracture energy of mortar and concrete by means of three point bend tests on notched beams. Mater Struct, **18 (4)**, 287-290 (1985).

[36] Beygi, M.H.A.: Kazemi, M.T.: Nikbin, I.M.: Amiri, J.V.: The effect of water to cement ratio on fracture parameters and brittleness of self-compacting concrete. Mater Des, **50**, 267-276 (2013).

[37] Madandoust, R.: Ranjbar, M.M.: Ghavidel, R.: Shahabi, S.F.: Assessment of factors influencing mechanical properties of steel fiber reinforced self-compacting concrete. Mater Des, **83**, 284-294 (2015).

[38] Ezeldin, A.S.: Balaguru, P.N.: Normal- and high-strength fiber-reinforced concrete under compression. ASCE J Mater Civ Eng, **4 (4)**, 415-429 (1992).

[39] Karadelis, J.N.: Lin, Y.: Flexural strengths and fibre efficiency of steel fibre- reinforced, roller-compacted, polymer modified concrete. Constr Build Mater, **93**, 498–505 (2015).

[40] Banthia, N.: Majdzadeh, F.: Wu, J.: Bindiganavile, V.: Fiber synergy in hybrid fiber reinforced concrete (HFRC) in flexure and direct shear. Cem Concr Compos, 48, 91–97 (2014).

[41] Banthia, N.: Nandakumar, N.: Crack growth resistance of hybrid fiber reinforced cement composites. Cem Concr Compos, **25 (1)**: 3–9 (2003).

[42] Markovic, I.: High-Performance Hybrid-Fibre Concrete: Development and Utilisation, IOS Press, 2006.

[43] Nataraja, M.C.: Dhang, N.: Gupta, A.P.: Stress-strain curves for steel-fiber reinforced concrete in compression. Cem Concr Comp, **21 (5-6)**, 383-390 (1999).

[44] Taerwe, L.: Gysel, A.: Influence of steel fibers on design stress-strain curve for high-strength concrete. J Eng Mech. **122**, 695-704. (1996).

[45] Abadel, A.: Abbas, H.: Almusallam, T.: Al-Salloum, Y.: Siddiqui, N.: Experimental and analytical investigations of mechanical properties of hybrid fiber reinforced concrete. Mag Concr Res, **68** (16), 823-843 (2016).

[46] Ibrahim, S.M.: Almusallam, T.H.: Al-Salloum, Y.A.: Abadel, A.A.: Abbas, H.: Strain rate dependent behavior and modeling for compression response of hybrid fiber reinforced concrete. Lat Am J Solids Struct, **13**, 1695-1715 (2016).

[47] Barros, J.A.O.: Cunha, V.M.C.F.: Ribeiro, A.F.: Antunes, J.A.B.: Post-cracking behavior of steel fibre reinforced concrete. Mater Struct, **38**, 47–56 (2005).

[48] RILEM TC 162-TDF, Test and design method for steel fibre reinforced concrete: σ–ε design method, Final recommendation. Mater Struct. **36(262)**, 560–7 (2003).

[49] RILEM TC 162-TDF, Test and design method for steel fibre reinforced concrete, Recommendation. Mater Struct. **33**, 3–5. (2000)

[50] Ernst, V.: Sohn. International Federation for Structural Concrete, fib Model Code for Concrete Structures, Berlin (2010).